Proceedings of the 8th World Congress on Mechanical, Chemical, and Material Engineering (MCM'22)
Prague, Czech Republic – July 31, 2022 - August 02, 2022
Paper No. HTFF 114
DOI: 10.11159/htff22.114

Experimental Investigation On Heat Transfer Enhancement And New Correlation Of Supercritical R1234ze(E) In Horizontal Helically Coiled Tube

Yi-Ran Jiang[1], Peng Hu[1,*], Qi Chen[1], Cheng-Qi Jia[1], Pan-Pan Zhao[2], Lei Jia[2]
[1] University of Science and Technology of China
Department of Thermal Science and Energy Engineering,Hefei, PR China
jiangyr@mail.ustc.edu.cn; hupeng@ustc.edu.cn; qichen17@mail.ustc.edu.cn; jcq@mail.ustc.edu.cn
[2]Hefei General Machinery Research Institute
Hefei, PR China
zhpp2016@163.com; magic9613@126.com

Abstract - HFOs refrigerant R1234ze(E) has been widely applied in supercritical heat pump system and supercritical Organic Rankine Cycle (ORC) in recent years due to zero ODP and extremely low GWP. In this paper, experimental research on the cooling heat transfer performances of supercritical HFO-1234ze(E) in horizontal helically coiled tube (HCT) is performed. The impacts of mass flux (G) and pressure (P) on the heat transfer coefficient (h), the relative proportion of gravitational buoyancy effect and centrifugal buoyancy effect (Ri_g / Ri_c), the heat transfer enhancement of HCT and the distribution of secondary flow velocity (V_s) are detailed analyzed. The increasing P suppresses the impact of G on h, while the increasing G strengthens the influence of P on h. Ri_g / Ri_c decreases with the enhancement of G, yet increases with the rising P. The higher the mass flux is, the more obvious the influence of centrifugal force on the cross-sectional distribution of V_s will be, and the more significant the heat transfer enhancement of HCT will become. When G is 240 and 400 kg/m^2 s respectively, h of s-R1234ze(E) in helical tube is 12.73% and 18.69% higher than that in straight tube. The variation of P hardly changes the centrifugal effect on the distribution of V_s, thus having little impact on the heat transfer enhancement of HCT. When P is 4.5 and 5 MPa respectively, h of helical tube is 15.38% and 15.12% higher than that of straight tube. In the region of T_b>T_{pc}, the correlation of straight tube has large prediction deviations for the performances of s-R1234ze(E) in helical tube owing to the absence of Ri_c term.

Keywords: s-R1234ze(E), helical tube, buoyancy effects, heat transfer enhancement, secondary flow, new correlation.

1. Introduction

In recent years, HFOs refrigerants have gained increasing attention owing to zero ODP, extremely low GWP, short lifetime in nature, and chemically stable property. R1234ze(E) is one of the widely-recognized HFOs refrigerants, which is considered as the most potential alternative to HFC-134a due to their similar thermo-physical properties. [1]

In the energy industry field, more and more attention has been concentrated on the application of supercritical fluid as heat transfer medium. Supercritical fluid can reach extremely high specific heat near pseudo-critical temperature (T_{pc}) and therefore can strengthen the heat transfer and greatly improve the energy utilization of thermal cycle system. Since the 1930s, numerous scholars have conducted researches on the convective heat transfer of refrigerants in straight tubes (ST) under supercritical pressure [2-4]. Compared with ST, the helically coiled tube (HCT) has compact structure and thus can save space. Moreover, the additional centrifugal force in HCT can generate centrifugal secondary flow in tube and further enhance the heat transfer. Therefore, helical heat exchanger tube has been widely adopted in recent years, and increasing attention has been focused on the supercritical heat transfer performances in HCT.

Zhang et al. [6] comparatively investigated the characteristics of sCO_2 flowing in ST and vertical HCT through experiments. Results showed that HCT has remarkable advantage in average heat transfer performance. Wang et al. [7] experimentally investigated the performances of sCO_2 in cooled horizontal HCT. The influence of buoyancy was explored by comparing h of upward and horizontal flows. Liu et al. [8] explored the influence of geometry of helical tube on h of sCO_2 through experiments. h of the tube with d=2 mm was three times that of the tube with d=4 mm and increased by 30%

with the decrease of coil diameter from 140 mm to 36 mm. Zhao et al. [9] adopted the SST $k-\omega$ model to simulate the turbulent flow of sH_2O in heated vertical HCT. The superposition of the buoyancy secondary flow and the centrifugal secondary flow resulted in the maximum V_s near the bottom being 17.6% higher than that near the top. Wang et al. [10] numerically analyzed the characteristics of supercritical methane in heated horizontal HCT under constant wall temperature with Reynolds Stress Model. The combined influences of buoyancy and centrifugal force led to the appearance of cold fluid at the outer-right region. Liu et al. [11] investigated the impacts of buoyancy and centrifugal force on the performances of sCO_2 in helical tubes under various inclination angles ($-90°$: $90°$) through simulation method. Zhang et al. [12] also employed the SST model to explore the flow patterns of sCO_2 in HCT and analyzed the buoyancy effect and flow acceleration effect.

As mentioned in the above literature, the advantages of helical heat exchanger tube are significant compared with ST. Although the researches on characteristics of supercritical fluids flowing in HCT have become increasingly sufficient, the majority of them still limited to inorganic refrigerants, and most of the correlations are only applicable to CO_2. Up to now, the investigation on the convective heat transfer performances of s-HFO-1234ze(E) in helical tube has been rarely published. Accordingly, the objective of the present work is to examine the performances of s-R1234ze(E) cooled in horizontal HCT through experiment to fill this gap.

2. Experiment

2.1. Experimental system

The experimental system (**Fig. 1**) had been described in detail in our previous study of straight tube [5], and only the heat exchanger tube of the test section has been replaced. R1234ze(E) from the gas cylinder flows into the cooling system after passing through the purifier and is cooled to liquid state with a temperature of about 6 °C . The subcooled R1234ze(E) is circulated by the high-pressure pump, and then enters the preheater to be heated to the preset temperature. After that, it goes into the test section to start the cooling process, and the cooling medium is silicon oil. Finally, the high temperature R1234ze(E) from the test section enters the sub-cooling loop to be cooled to room temperature, and then a full cycle is completed. The operating pressure is regulated by the pressure regulating valve. The flow rate and the inlet temperature of the helical tube are manually controlled by the high-pressure variable speed gear pump and the preheater, respectively. The flow rate of HFO-1234ze(E) is measured by the flowmeter installed before the high-pressure pump with an accuracy of ± 1%. The inlet and outlet pressures of the test section are measured by pressure sensors with an accuracy of ±0.1%FS. T-type thermocouples (accuracy: ±0.1 °C) are respectively arranged at the inlet and outlet of the helical tube and the shell tube, and 12 temperature measuring points on the outer wall of the helical tube.

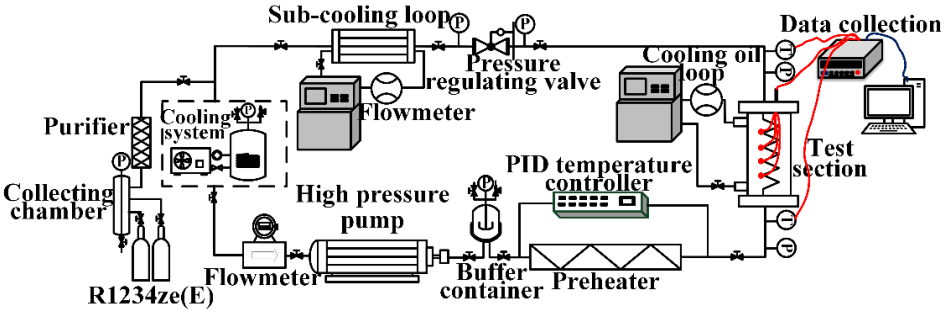

Fig. 1. Schematic diagram of the experimental system.

The test section is a tube-in-tube heat exchanger, with the refrigerant and the silicon oil respectively flowing inside the inner helical tube and the shell tube, as presented in **Fig. 2**. The helical tube and shell tube are both made of 316 stainless steel. The coil pitch, coil radius, inner diameter, and outer diameter of the helical tube are 25 mm, 20 mm, 4 mm, and 6 mm, respectively. The total helical length is about 700 mm, corresponding to about 5 turns of helical coils. The distributions of thermocouples for wall temperature measurement are presented in **Fig. 3**. A total of 12 thermocouples are adopted to measure the outer wall temperature.

Fig. 2. Picture of the test section.

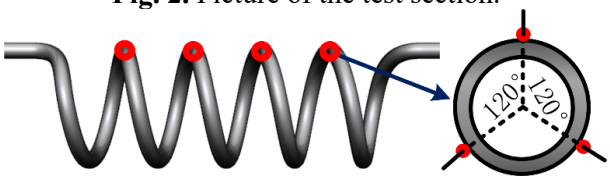

Fig. 3. The distributions of thermocouples for wall temperature measurement.

2.2. Data processing

In the process of the experiment, firstly, the system pressure and the flow rate of R1234ze(E) are controlled by adjusting the pressure regulating valve and the speed of high-pressure pump. After that, the inlet temperature of the helical tube is set at 420 K by regulating the preheater. Then, the inlet temperature of the cooling silicon oil needs to be adjusted to an appropriate value to guarantee that the difference of the inlet and outlet temperatures of the refrigerant can be maintained within a small range. Therefore, the average h of the heat exchange section can be determined by the ratio of the average q to the difference between the average temperatures of the refrigerant and the inner wall. Finally, the inlet temperature of the helical tube will be gradually reduced to obtain a series of heat transfer coefficients in the whole temperature range (365-420 K).

$$q = \dot{m}_R (i_{in} - i_{out}) / \pi d_i L \tag{1}$$

$$T_{inner-wall} = T_{outer-wall} + Q_R In\left(d_o / d_i\right) / 2\pi L\lambda = \left(T_1 + T_2 + \cdots + T_{12}\right) / 12 + Q_R In\left(d_o / d_i\right) / 2\pi L\lambda \tag{2}$$

$$h = q / \left(T_R - T_{inner-wall}\right) = q / \left[\left(T_{in,R} + T_{out,R}\right) / 2 - T_{inner-wall}\right] \tag{3}$$

Where $\dot{m}_R$ and T_R represent the mass flow rate and the average temperature of R1234ze(E). i_{in}, i_{out}, $T_{in,R}$ and $T_{out,R}$ are respectively the inlet and outlet enthalpies and temperatures of HFO-1234ze(E). L, d_i and d_o are the total helical length and inner and outer diameters of the helical tube. λ represents the thermal conductivity of the 316 stainless steel.

Since the difference of the inlet and outlet temperatures of HFO-1234ze(E) is maintained to be very small, q is only 5-15 kW/m^2. In this work, G ranges from 160 to 400 kg/m^2 s, P ranges from 4 to 5 MPa, and the fluid temperature ranges from 365 to 420 K. The calculation of the uncertainties of experimental data had been expounded in our previous work [5]. The maximum uncertainties of q, $T_{inner-wall}$, and h in the present work are ± 11.73 %, ± 0.126 °C, and ± 12.25 %, respectively.

2.3. Validations of experimental results

To verify the reliability of the experimental system, the cooling process of s-HFO-1234ze(E) in HCT is numerically simulated. The simulation method, boundary conditions and mesh generation method are the same as our previous research [5]. Besides, the geometric parameters of the physical model are all consistent with those in the experiment. In the present

work, the heat flux ranges from 5-15 kW/m^2, thus the influence of q can be neglected since the effect of q on h is negligible under the condition of low heat flux [5]. Hereinafter, the simulation results of HCT with q=10 kW/m^2 are selected to validate the experimental accuracy. As can be observed in **Fig. 4**, the variation trends of experimental results agree well with the numerical results. The average absolute deviations of h are 13.31% and 12.14%, respectively, indicating that the experimental system has high reliability.

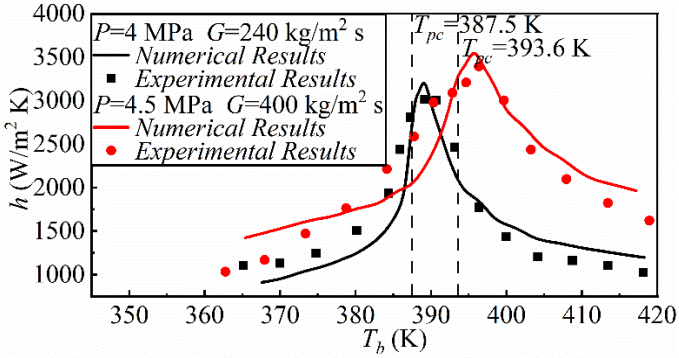

Fig. 4. Comparisons between experimental and numerical results.

3. Results and discussion

3.1 Effects of mass flux on heat transfer performance and buoyancy

Fig. 5 illustrates the effects of G on h when P is 4 and 4.5 MPa, respectively. With the rise of G from 160 to 400 kg/m^2 s, the Reynolds number of s-R1234ze(E) increases, resulting in thinner boundary layer and higher turbulence intensity. Consequently, the heat transfer capacity enhances in the whole bulk temperature range. When P is 4 MPa, the peak value of h increases about 2800 W/m^2 K with the rise of G from 160 to 400 kg/m^2 s, while when P is 4.5 MPa, the peak value only increases about 1800 W/m^2 K, indicating that the influence of G on heat transfer performance is suppressed by the increasing P. At lower P, the thermos-physical properties (especially the specific heat) of s-R1234ze(E) vary more sharply near T_{pc}, resulting in smaller temperature difference between the wall and the core fluid, which causes h more sensitive to the variation of G.

As is well known that the buoyancy has significant influences on the flow field and thermal field distributions of supercritical fluid. In helical tube, both the gravitational buoyancy induced by gravity and the centrifugal buoyancy induced by additional centrifugal force exist. The gravitational Richardson number (Ri_g) and centrifugal Richardson number (Ri_c) can both be expressed in the form of Gr / Re^2:

$$Ri_g = Gr_g \Big/ Re_b^2 = (\rho_w - \rho_b)\rho_b g d^3 \Big/ \left(\mu_b^2 g Re_b^2\right) \tag{4}$$

$$Ri_c = Gr_c \Big/ Re_b^2 = u^2(\rho_w - \rho_b) d^3 \Big/ \left(R\rho_b v_b^2 g Re_b^2\right) = 2\delta(\rho_w - \rho_b)/\rho_b \tag{5}$$

In this work, Ri_g / Ri_c is introduced to explore the relative proportion of the influences of gravitational buoyancy and centrifugal buoyancy on heat transfer. **Fig. 6** presents the profiles of Ri_g / Ri_c under different G when P is 4 and 4.5 MPa, respectively. With the increase of T_b, Ri_g / Ri_c decreases, illustrating that the gravitational buoyancy plays a dominant role at low temperature, while the centrifugal buoyancy effect is relatively strong in the high-temperature region. When G increases from 160 to 400 kg/m^2 s, the acceleration of fluid will lead to the weakening of gravitational buoyancy and the enhancement of centrifugal buoyancy, hence the value of Ri_g / Ri_c decreases. Furthermore, when P rises from 4 to 4.5

MPa, due to the rightward shift of the critical point, the bulk temperatures corresponding to Ri_g / Ri_c=1 become larger.

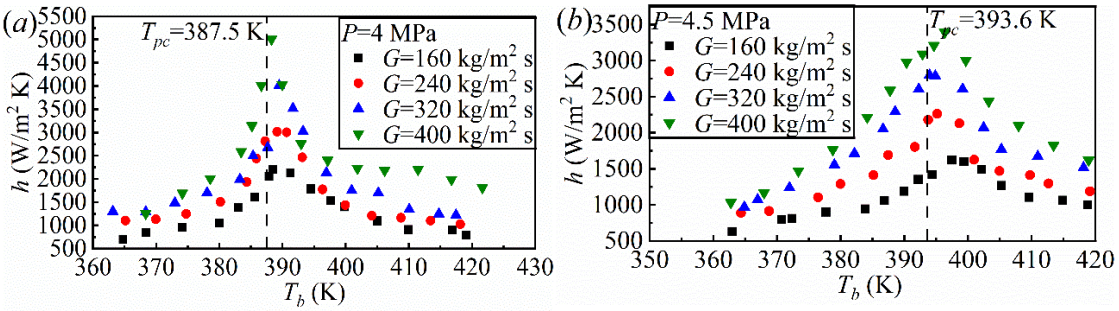

Fig. 5. Effects of G on h under different P. (a) P=4 MPa, (b) P=4.5 MPa.

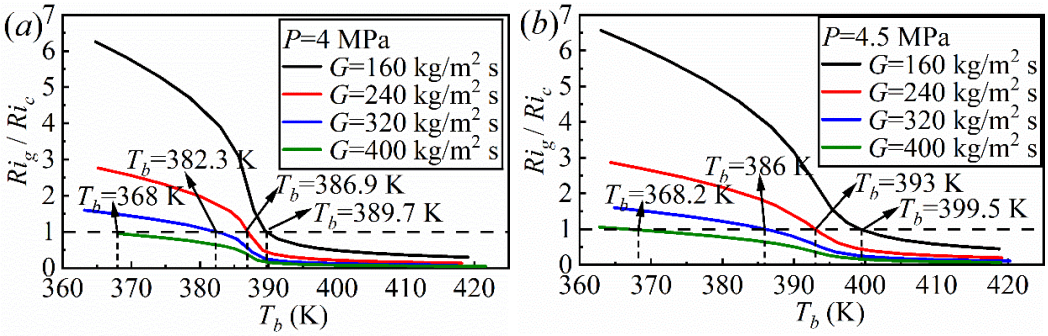

Fig. 6. Effects of G on Ri_g / Ri_c under different P. (a) P=4 MPa, (b) P=4.5 MPa.

3.2 Effects of pressure on heat transfer performance and buoyancy

Fig. 7 illustrates the influences of P on h when G is 240 and 320 kg/m² s, respectively. The maximum value of h drops and moves to the right with the rise of P, which is consistent with the variation of the peak value of specific heat with pressure. Before T_b=390 K, the increasing P leads to lower heat transfer coefficient, yet opposite conclusion can be obtained after T_b=400 K. When the G is 240 kg/m² s, the peak value of h drops about 1100 W/m² K with the increase of P from 4 to 5 MPa; while when G is 320 kg/m² s, the peak value reduces about 1600 W/m² K, which demonstrates that the influence of P on h is strengthened by the increasing G. Similar to the analysis in **section 3.1**, the turbulence intensity of s-R1234ze(E) is higher and the fluid mixing in cross-section is more intense at higher G, resulting in more uniform temperature distribution in tube; consequently, the difference between the wall temperature and the bulk temperature is smaller, which causes h more sensitive to the variation of P.

Fig. 8 presents the values of Ri_g / Ri_c under different P when G is 240 and 320 kg/m² s, respectively. The density of s-R1234ze(E) varies more gently with temperature under higher P, which leads to more uniform density distribution in cross-section with the same T_b. Consequently, with the rise of P, both the gravitational buoyancy and the centrifugal buoyancy will be weakened. In **Fig. 9**, the value of Ri_g / Ri_c increases with P, indicating that the weakening of centrifugal buoyancy is more rapidly than that of the gravitational buoyancy. Moreover, when G increases from 240 to 320 kg/m² s, owing to the decrease of Ri_g / Ri_c, the bulk temperatures corresponding to Ri_g / Ri_c=1 will reduce.

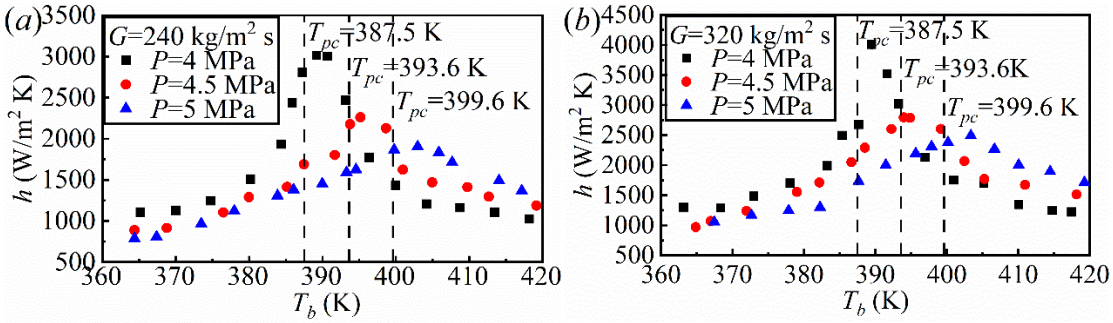

Fig. 7. Influences of P on h under different G. (*a*) G=240 kg/m^2 s, (*b*) G=320 kg/m^2 s.

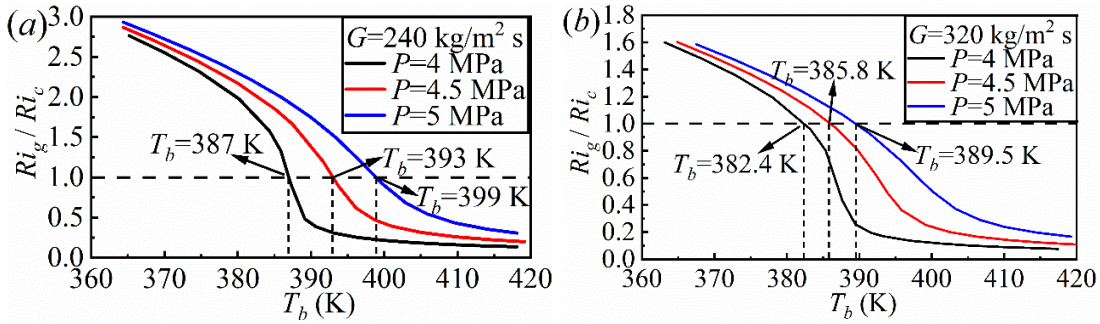

Fig. 8. Influences of P on Ri_g / Ri_c under different G. (*a*) G=240 kg/m^2 s, (*b*) G=320 kg/m^2 s.

3.3 Heat transfer enhancement of HCT

The centrifugal secondary flow generated by the additional centrifugal force in the cross-section of HCT can enhance the mixing degree of the near-wall fluid and the core fluid, thus can greatly improve the convective heat transfer of ST. In this section, the experimental data of horizontal HCT and ST with the same diameter under four different conditions are selected for comparisons. The data of ST are acquired from our previous experimental study [5]. **Fig. 9 (*a*)** presents the influence of G on heat transfer enhancement of HCT. When G is 240 kg/m^2 s, h of HCT is 12.73% higher than that of ST on average; while when G is 400 kg/m^2 s, the gap of h between HCT and ST increases to 18.69% on average, indicating that the heat transfer enhancement of HCT is more significant at higher G. **Fig. 9 (*b*)** presents the comparisons of h between HCT and ST under different P. When P is 4.5 and 5 MPa respectively, h of HCT is 15.38% and 15.12% higher than that of ST on average, which demonstrates that the variation of P has almost no impact on the heat transfer enhancement of HCT.

To better analyze the above conclusions, the secondary flow velocity (V_s) distributions at T_b=T_{pc} of HCT and ST under different working conditions are compared. In **Fig. 10 (*a*)**, when G is 240 kg/m^2 s, the centrifugal secondary flow generated by the helical structure leads to the increase of the maximum V_s from 0.012 m/s to 0.095 m/s; whereas when G is 400 kg/m^2 s, the maximum V_s increases from 0.0085 m/s to 0.17 m/s. Therefore, the higher the mass flux is, the more obvious the influence of centrifugal force on the secondary flow velocity distribution will be, and the greater the increment of h will become. In **Fig. 10 (*b*)**, when P is 4.5 MPa, the maximum V_s in the cross-sections of T_b=T_{pc} of HCT and ST are 0.13 m/s and 0.012 m/s, respectively; when P is 5 MPa, the maximum V_s are 0.13 m/s and 0.011 m/s, respectively. It can be concluded that the variation of P hardly changes the centrifugal effect on the secondary flow velocity, consequently, the increment of h will be basically unchanged.

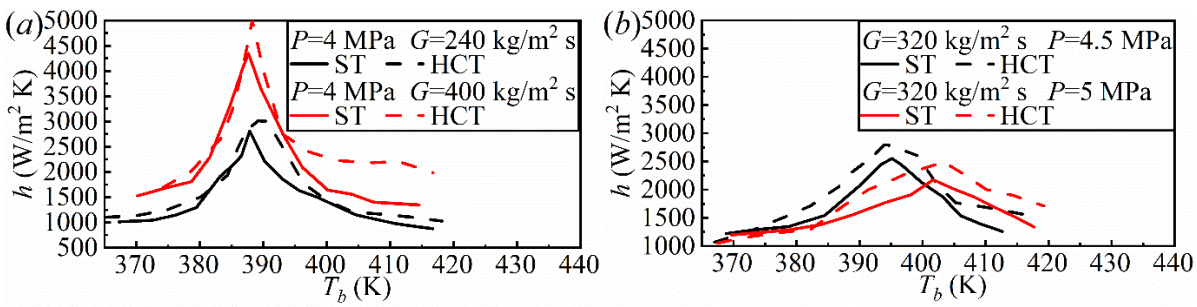

Fig. 9. Comparisons of h between HCT and ST under (a) different G and (b) different P.

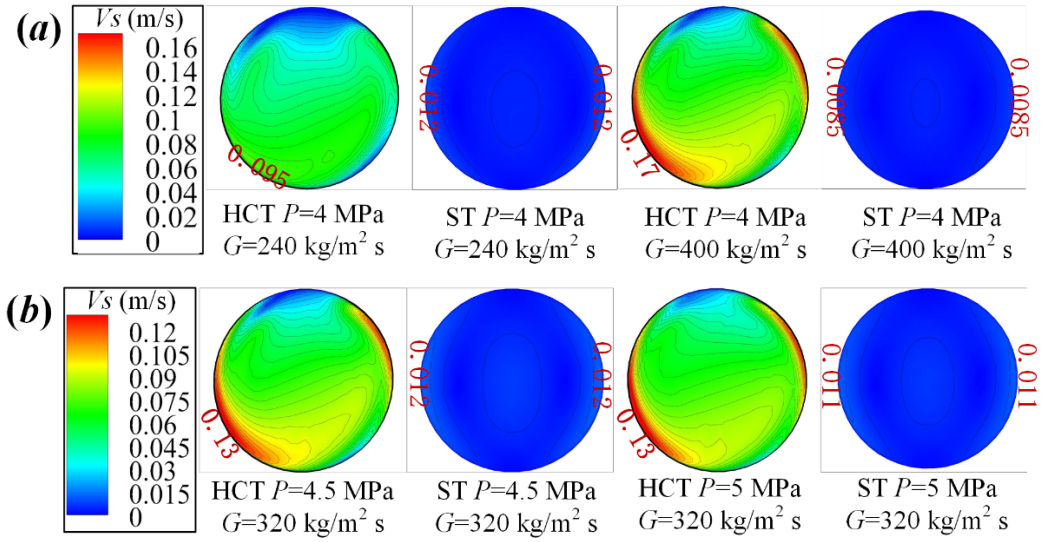

Fig. 10. V_s of HCT and ST at T_b=T_{pc} under (a) different G and (b) different P.

3.4 New correlation of Nusselt number for s-R1234ze(E) in HCT

In our previous experimental research, the convective heat transfer correlation of s-HFO-1234ze(E) in horizontal ST had been developed [5]:

$$\begin{aligned} T_b < T_{pc}&: \quad Nu_b = 0.001\, Re_b^{1.22}\, Pr_b^{0.692} \left(\rho_b/\rho_w\right)^{3.139} \left(\overline{c}_p/c_{p,w}\right)^{0.03} Ri_g^{0.226} \\ T_b \geq T_{pc}&: \quad Nu_b = 0.0027\, Re_b^{1.037}\, Pr_b^{0.396} \left(\rho_b/\rho_w\right)^{-0.31} \left(\overline{c}_p/c_{p,w}\right)^{-0.062} Ri_g^{0.106} \end{aligned} \tag{6}$$

Firstly, the experimental results of s-R1234ze(E) in HCT (Nu_{exp}) are compared with the Nusselt numbers calculated by the straight tube correlation (Nu_{cal}), as presented in **Fig. 11**. When T_b<T_{pc}, the values of Nu_{cal} / Nu_{exp} are almost within the range of 0.8-1.2, while when T_b>T_{pc}, most of the values are beyond the range of 0.8-1.2. This indicates that the heat transfer correlation of ST is appropriate to be used to predict the performance of s-HFO-1234ze(E) in HCT in the low-temperature region, whereas for the high-temperature region, the prediction results of the straight tube correlation have large deviations. As can be seen from **Figs. 6 and 8**, the values of Ri_g / Ri_c are almost basically less than 1 when T_b>T_{pc}, which means that the influence of gravitational buoyancy is relatively weak, while the centrifugal buoyancy effect cannot be neglected in this region. Since there is no centrifugal buoyancy term in the correlation of ST, it is impossible to accurately predict the heat transfer of the fluid in HCT in the high-temperature region.

Then, in this work, a new correlation is obtained by adding the centrifugal buoyancy term (Ri_c):

$$\begin{aligned} T_b < T_{pc}:\ \ Nu_b &= 1.321\times10^{-15}\, Re_b^{3.564}\, Pr_b^{2.14} \left(\rho_b/\rho_w\right)^{-0.717} \left(\overline{c}_p/c_{p,w}\right)^{-3.829} Ri_g^{1.493} Ri_c^{-1.857} \\ T_b \geq T_{pc}:\ \ Nu_b &= 2.661\times10^{-9}\, Re_b^{2.074}\, Pr_b^{0.399} \left(\rho_b/\rho_w\right)^{-4.066} \left(\overline{c}_p/c_{p,w}\right)^{-0.613} Ri_g^{0.682} Ri_c^{-1.52} \end{aligned} \tag{7}$$

Fig. 11 also presents the comparisons between Nu_{exp} obtained from the cooling heat transfer experiment of HCT and Nu_{cal} calculated from the above new correlation. In both the sections of $T_b<T_{pc}$ and $T_b>T_{pc}$, the values of Nu_{cal}/Nu_{exp} are always within the range of 0.85-1.15. Consequently, the new correlation can be employed to accurately predict the cooling performances of s-R1234ze(E) in HCT.

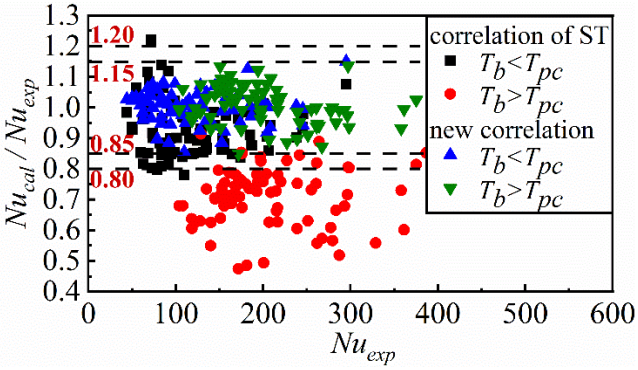

Fig. 11. Comparisons of the experimental *Nu* with those calculated by the correlation of ST and the new correlation.

4. Conclusions

The performances of s-HFO-1234ze(E) in cooled horizontal HCT are experimentally investigated. The influences of *P* and *G* on *h*, buoyancy effects and heat transfer enhancement of HCT are detailed analyzed. The main conclusions can be summarized:

(1) The increasing *P* will suppress the influence of *G* on *h*. The gravitational buoyancy plays a leading role at low temperature, while the centrifugal buoyancy effect is more significant in the high-temperature region. When *G* increases, the weakening of gravitational buoyancy and the enhancement of centrifugal buoyancy will lead to the decrease of Ri_g/Ri_c.

(2) The increasing *G* will strengthen the influence of *P* on *h*. With the rise of *P*, both the gravitational buoyancy and the centrifugal buoyancy will be weakened. However, the weakening of centrifugal buoyancy is more rapidly than that of the gravitational buoyancy, thus the value of Ri_g/Ri_c increases.

(3) The higher the mass flux is, the more obvious the influence of centrifugal force on the secondary flow velocity distribution will be, and the more significant the heat transfer enhancement of HCT will become. The variation of *P* hardly changes the centrifugal effect on the secondary flow velocity and therefore has almost no impact on the heat transfer enhancement of HCT.

(4) In the region of $T_b>T_{pc}$, the correlation of straight tube has large prediction deviations for the performances of s-R1234ze(E) in helical tube owing to the absence of Ri_c term. The new heat transfer correlation with the centrifugal buoyancy term can accurately predict the cooling performances of s-HFO-1234ze(E) in horizontal HCT in both the sections of $T_b<T_{pc}$ and $T_b>T_{pc}$, and the deviations are both within $\pm15\%$.

Acknowledgments

This work is supported by the National Natural Science Foundation of China (Grant No.: 52176171), Anhui Provincial Key Research and Development Program (Grant No.: 202004a07020017).

References

[1] Mota-Babiloni, A., Navarro-Esbri, J., Moles, F., Cervera, A. B., Peris, B., and Verdu, G., 2016, "A review of refrigerant R1234ze(E) recent investigations," Appl. Therm. Eng., 95(1), pp. 211-222.

[2] Xie, J. Z., Liu, D. C., Yan, H. B., and Xie, G. N., 2020, "A review of heat transfer deterioration of supercritical carbon dioxide flowing in vertical tubes: Heat transfer behaviors, identification methods, critical heat fluxes, and heat transfer correlations," Int. J. Heat Mass Transf., 149(1), pp. 119233.

[3] Ehsan, M. M., Guan, Z. Q., and Klimenko, A. Y., 2018, "A comprehensive review on heat transfer and pressure drop characteristics and correlations with supercritical CO_2 under heating and cooling applications," Renew. Sust. Energ. Rev., 92(1), pp. 658-675.

[4] Xie, J. Z., Yan, H. B., and Sunden, B., 2019, "A numerical prediction on heat transfer characteristics from a circular tube in supercritical fluid crossflow," Appl. Therm. Eng., 153(1), pp. 692-703.

[5] Jiang, Y. R., Hu, P., 2020, "Experimental and numerical investigation on heat transfer characteristics of supercritical R1234ze(E) cooled in horizontal tubes," Int. J. Heat Fluid Flow, 85(1), pp. 108650.

[6] Zhang, S. J., Xu, X. X., Liu, C., Liu, X. X., and Dang, C. B., 2020, "Experimental and numerical comparison of the heat transfer behaviors and buoyancy effects of supercritical CO_2 in various heating tubes," Int. J. Heat Mass Transf., 149(1), pp. 119074.

[7] Wang, K. Z., Xu, X. X., Liu, C., Bai, W. J., and Dang, C. B., 2017, "Experimental and numerical investigation on heat transfer characteristics of supercritical CO_2 in the cooled helically coiled tube," Int. J. Heat Mass Transf., 108(B), pp. 1645-1655.

[8] Liu, X. X., Xu, X. X., Liu, C., He, J. C., and Dang, C. B., 2019, "The effect of geometry parameters on the heat transfer performance of supercritical CO_2 in horizontal helically coiled tube under the cooling condition," Int. J. Refrig., 106(1), pp. 650-661.

[9] Zhao, H. J., Li, X. W., and Wu, X. X., 2017, "Numerical investigation of supercritical water turbulent flow and heat transfer characteristics in vertical helical tubes," J. Supercrit. Fluids, 127(1), pp. 48-61.

[10] Wang, C. G., Sun, B. K., Lin, W., He, F., and You, Y. Q., 2018, "Turbulent convective heat transfer of methane at supercritical pressure in a helical coiled tube," J. Therm. Sci., 27(1), pp. 55-63.

[11] Liu, X. X., Xu, X. X., Liu, C., Ye, J., Li, H. R., Bai, W. J., and Dang, C. B., 2017, "Numerical study of the effect of buoyancy force and centrifugal force on heat transfer characteristics of supercritical CO_2 in helically coiled tube at various inclination angles," Appl. Therm. Eng., 116(1), pp. 500-515.

[12] Zhang, S. J., Xu, X. X., Liu, C., Zhang, Y. D., and Dang, C. B., 2018, "The buoyancy force and flow acceleration effects of supercritical CO_2 on the turbulent heat transfer characteristics in heated vertical helically coiled tube," Int. J. Heat Mass Transf., 125(1), pp. 274-289.